Nanotechnology Perceptions
ISSN 1660-6795
www.nano-ntp.com

A synergistic approach of the application of Nanoparticles and Ionic Liquid for designing Drilling Fluids for Shale Formation

Gauri Sankar Bora[a], Prasenjit Talukdar[b*], Jiban Saikia[c], Tamanna Kashyap[b], Tanmay Chakraborty[b], Tridip Lahkar[b], Tushar Poddar[b], Biki Boruah[b], Gaurav Himanta Khaklari[a]

[a] *Department of Petroleum Technology, Dibrugarh University, Dibrugarh-786004, Assam, India*
[b] *Department of Petroleum Engineering, DUIET, Dibrugarh University, Dibrugarh-786004, Assam, India*
[c]*Department of Chemistry, Dibrugarh University, Assam, 786004, India*
**Corresponding author's email address: prasenjit_duiet@dibru.ac.in*

The drilling fluids play a major role in the oil and gas industry for cuttings conveyance, drill bit cooling, and wellbore stability. This paper presents an enhanced water-based drilling fluid with silicon dioxide nanoparticles, multiwall carbon nanotubes, and the ionic liquid 1-Methyl-3-Octylimidazolium chloride. These additives help ensure that this fluid has low viscosity at extreme low shear rates and has shear-thinning behavior so that it can suspend the cutting efficiently at low flow, provides reduced resistance at higher shear rates, and saves energy in pumping. The ionic liquid increases the viscosity profile by making it responsive to all kinds of drilling conditions. Shear stress measurements indicate specific samples show little shear rate dependency, such as SiO_2 (0.25%) + Ionic fluid (0.03%) sample at 0.286 Pa with 0.1 1/s or SiO_2 (0.25%) + Ionic fluid (0.05%) sample at 0.09531 Pa with 0.1 1/s. MWCNT (0.25%) + Ionic fluid (0.07%) sample shows increased resistance; it rises significantly in shear stress from approximately 87.131 Pa at 0.1 1/s to around 518.44 Pa at 100 1/s, probably because of the increased concentration of nanoparticle or ionic liquid. It offers adjustable viscosity and shear stress, thus applicable for shale drilling, supports effective flow control, minimizes formation damage, and enhances efficiency in the high-pressure and high-temperature environment.

Keywords: Ionic liquids; Nanoparticle-enhanced drilling fluids; Rheological properties; Shale drilling; Shear-thinning behavior

Abbreviations

WBDF - Water-Based Drilling Fluids
CoF - Coefficient of Friction
GBs - Glass Beads
BMIM-Cl - 1-Butyl-3-Methylimidazolium Chloride
API - American Petroleum Institute
SiO_2 - Silicon Dioxide
MWCNT - Multi-Walled Carbon Nanotube
ILs - Ionic Liquids
WBM - Water-Based Mud
XC Polymer - Xanthan Gum Polymer
$CaCO_3$ - Calcium Carbonate
PAC-R - Polyanionic Cellulose (Regular)
PAC-L - Polyanionic Cellulose (Low-Viscosity)
PGS - Polyglycol Synthetic
KCl - Potassium Chloride
[OMIM]+[Cl]- - 1-Methyl-3-Octylimidazolium Chloride
NMR - Nuclear Magnetic Resonance
^{1}H NMR - Proton Nuclear Magnetic Resonance
^{13}C NMR - Carbon-13 Nuclear Magnetic Resonance
PAC-R - Polyanionic Cellulose - Regular
PAC-L - Polyanionic Cellulose - Low viscosity
Gel_0 - Initial Gel Strength
Gel_{10} - Gel Strength after 10 minutes
XC Polymer - Cross-linked Polymer
KCl - Potassium Chloride

Symbols

°C - Degrees Celsius (temperature unit)
g/100mL - Grams per 100 Milliliters (concentration)
% - Percent (proportion)
+/- - Positive/Negative charge in ionic forms (e.g., [OMIM]+[Cl]-)
µm - Micrometer (unit of length)
ppb - Parts Per Billion (unit of concentration)
ml - Milliliters (unit of volume)
psi - Pounds Per Square Inch (unit of pressure)
1/32 inch - Fractional representation of an inch (1/32 inch = approx. 0.79375 ml)
PPG - Pounds per Gallon
Gm/CC - Grams per Cubic Centimeter
Lb/feet^3 - Pounds per Cubic Foot
Lb/inch^2/1,000 ft - Pounds per Square Inch per 1,000 Feet
cP – Centipoise
mm – Millimeters

μm – Micrometers
δ - Chemical shift in NMR spectroscopy
J - Coupling constant in Hz (Hertz)
s - Singlet (NMR peak splitting pattern)
d - Doublet (NMR peak splitting pattern)
t - Triplet (NMR peak splitting pattern)
m - Multiplet (NMR peak splitting pattern)
dyne/cm² - Dynes per square centimeter (for gel strength)
mPa·s - Millipascal-second (unit of viscosity)
Pa - Pascal (unit of pressure or stress)
tan δ - Loss factor (ratio of viscous to elastic components in a fluid)
1/s - Per second (unit of shear rate)

1. Introduction

Shales are highly dense, fine-grained sedimentary rocks composed of clay minerals, quartz, and organic matter (Lundegard & Samuels, 1980). Their high content of hydrocarbon makes them a very valued source in oil and gas production (Zou et al., 2019). However, these characteristic poses unique challenges while drilling through shale formations. They have a tendency to absorb water and swell that gives rise to instability in the formation. Such high-fine-grained characteristics of shale and its very low permeability may restrict fluid flow, complicating the drilling process and further enhance the risk of instability of the wellbore (Kamali et al., 2021)(Muhammed et al., 2021). One of the primary issues that occur while drilling through shale formations is the reactivity of shale with conventional water-based drilling fluids. Water causes hydrates to swell and break down the shale. This reactivity not only causes wellbore collapse but also complicates drilling and often requires interventions in these shale formations. Normally, they are penetrated at great depths and high temperatures, which affects the efficiency of drilling fluids and results in thermal degradation with gradual loss of fluid properties.

Drilling fluids offer the ability to overcome difficult challenges, including wellbore stability, enhance rheology, fluid loss control, cooling the drill bit, and cuttings removal to the surface (Talukdar, 2017)(Talukdar et al., 2018)(Talukdar & Gogoi, 2015). Traditional water-based drilling fluids often lack shale inhibition, and often do not allow for appropriate lubrication while oil-based fluids provide much better shale stability but, in many cases, can be environmentally and financially drawbacks, including increased costs as well as stricter disposal regulations (Gao, 2024). Several alternative formulations have therefore been developed that would find a balance between shale stability, environmental safety, and a reasonably cost such as XC-Polymer, brine-base drilling fluid, (Blkoor & Ka, 2013)(Xia & Pan, 2023).

Advanced additives, therefore, include nanoparticles and ionic liquids, which have been used to improve the performance of drilling fluid (Aftab et al., 2017)(Rahman et al., 2020). Nanoparticles are small in size and, therefore, offer a high surface area with which they penetrate the shale pores, helping in providing a barrier where swelling of the shale is inhibited (Bayat & Shams, 2019).Due to the higher surface area and chemical stability of nanoparticles and improvement of fluid properties at relatively low concentrations, particles usually in the range of 1-100 nanometers provide a number of benefits from a drilling fluids perspective.

Important advantages derived from nanoparticle application include stabilization of shale formations. Due to their small diameter, it allows them to penetrate pore and micro-fracture spaces within the shale structure. In addition, nanoparticle slurries create physical barrier resistance for water infiltration, reducing shale swelling to facilitate stabilization in the borehole wall. Nanoparticles enhance rheological behavior of drilling fluids, that is, yield stress viscosity improving, important in suspending carrying drilling cuttings back to surface. They also control filtration by creating a thin impermeable layer on the wellbore wall that minimizes fluid loss and reduces instability in the wellbore. Nanoparticles are thermally stable. Hence, drilling fluids perform the same way at any high temperature at which traditional additives break down. Ismail et al. (2016) studied the impacts of MWCNT, nanosilica, and glass beads (GBs) on the rheological properties, filtrate volume, and lubricity of WBDF. The varied concentrations of MWCNT and nanosilica (0.001 to 0.2 ppb) and GBs of varying sizes (90–150 μm and 250–425 μm) at concentrations from 2 to 12 ppb were tested. The results showed that the 0.01 ppb of MWCNT and nanosilica decreased coefficient of friction (CoF) by 44% and 38%, respectively, and the 4 ppb of smaller GBs resulted in a 28% decrease in CoF; moreover, MWCNT obtained a filtrate volume of 4.5 ml and mud cake thickness of 2/32 inch (Ismail et al., 2016).

Ionic liquids are salts that exist in a liquid state and have properties such as thermal stability, low volatility, and tunable chemical structures. These properties make ionic liquids extremely beneficial for use in drilling fluids, particularly in challenging shale formations. Liquid salts improve shale stability by creating a protective layer on the shale surfaces that prevents swelling and reduces water reactivity. These properties are most beneficial to drilling operations in water-sensitive formations, where swelling can destabilize the wellbore. There are several other benefits of the use of ionic liquids in drilling fluids, including effective lubrication, which minimizes the friction between the drill pipes and the wellbore, retention of performance at high temperatures, and some environmental benefits due to relatively less toxicity and higher biodegradability compared to those oil-based fluids. Luo et al. (2017) investigated the impact of a water-soluble ionic liquid on the rheological and filtration properties of water-based drilling fluids at high temperatures. They conducted rheological and filtration tests according to API standards, including high-temperature aging processes. Results demonstrated that adding a low concentration of ionic liquid (0.05%) significantly improved fluid stability and reduced filtration volumes by up to 52% under high-temperature, high-pressure conditions (Luo et al., 2017). Ofei et al. (2017) explored the effects of 1-butyl-3-methylimidazolium chloride (BMIM-Cl) on the rheological and filtration properties of water-based drilling mud at temperatures from 25°C to 200°C and a pressure of 1000 psi. They conducted tests following API standards and applied three rheological models—Bingham Plastic, Power Law, and Herschel–Bulkley—to describe the mud behavior. Results showed that BMIM-Cl improved mud stability, viscosity, and filtration control, with the Herschel–Bulkley model best describing the shear-thinning behavior, highlighting BMIM-Cl's potential as a drilling mud additive for high-temperature wells (Ofei et al., 2017). The combination of nanoparticles and ionic liquids in drilling fluids provides a synergistic approach to enhanced shale stability, reduced environmental impact, and improved drilling efficiency. Innovative additives address problems such as wellbore instability, fluid loss, and high thermal demands in shale formations. Nanoparticles enhance rheology and filtration control, while ionic liquids

provide enhanced lubrication, thermal stability, and shale inhibition. The novel combination has huge potential as it offers high-performance sustainability in drilling fluids and creates promising ways toward shale drilling solutions that will prove to be more effective.

2. MATERIALS AND METHODS

2.1. Selection of Nanoparticles and Ionic Liquids

The nanoparticles and the ionic liquids were chosen in this paper based on their compatibility with drilling fluids, as well as their efficiency toward shale stabilization and thermal stability. Normally, nanoparticles typically used include SiO_2 and multi-walled carbon nanotube (MWCNT), because they exhibit high surface areas and have proven stability in drilling processes. Ionic liquids such as imidazolium-based and ammonium-based ILs, because of low toxicity and excellent resistance to high temperatures, have been chosen for good shale-inhibitive behavior as well as friction diminution.

2.2. Synthesis of Ionic Liquid

In a round-bottom flask, 1-methylimidazole (2 g, 24.39 mmol) and 1-chlorooctane (3.9 g, 26.82 mmol) were combined with acetonitrile as the solvent. The reaction was carried out in a condenser-fitted round-bottom flask at 80°C for approximately 10 to 15 hours. Upon completion of the reaction, two distinct layers were observed. The ionic liquid (IL) layer was collected, and it was then washed repeatedly with ethyl acetate to remove any excess 1-chlorooctane. The residual layer obtained from this process was identified as [OMIM][Cl].

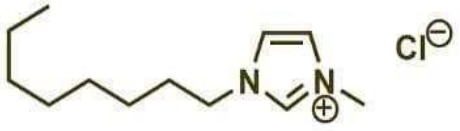

Figure 1. 1-Methyl-3-Octylimidazolium chloride ([OMIM]+[Cl]-)

2.3. Characterization of Nanoparticles

The formation of ZnO nanoparticles was examined using X-Ray Diffraction (XRD). The XRD peaks were obtained with an X-ray diffractometer operating at 40kV/30mA. To study the morphology and structural characteristics of the ZnO sample, a Scanning Electron Microscope (SEM) was utilized. This technique was also employed to determine the nanoparticle size. SEM functions by directing a focused electron beam across the sample, producing high-resolution surface images.

2.4. Preparation of Drilling Fluid Formulations

The nanoparticle concentration and ionic liquid concentration were varied over a wide range in base water-based fluids. The dispersed nanoparticles were made through high-speed mixing

to ensure good homogeneity of the particles within the fluid. The prepared fluids rested for some time after blending with ionic liquids for stabilization before the experiment was performed. The optimization parameters involved concentration of nanoparticles, the ionic liquid to base fluid ratio, as it plays a key role in optimizing shale stability along with rheological properties.

Table 1. Components of the base mud and constituent additives

Name of the component	Properties (Base fluid and additives for WBM)	Concentration % (g/100mL)
Water	Continuous phase	
XC Polymer	Bridging agent, Rheological improvement	1
$CaCO_3$	Weighting Agent, Plugging material, pH control	6
PAC-R		1
PAC-L	Fluid loss control	1
PGS		2.5
KCl	Shale inhibition	5
SiO_2	Nanoparticle	0.05/ 0.15/ 0.25
MWCNT	Nanoparticle	0.05/ 0.15/ 0.25
$[OMIM]^+[Cl]^-$ (liquid state)	Ionic fluid	0.03/0.05/0.07/0.09/0.11
Formaldehyde	Biocide	0.1

In this formulation, XC Polymer is added at 1% as bridging agent, boosting the viscosity for better cuttings transport and preventing phase separation under various drilling conditions. The calcium carbonate at 6% serves as a weighting agent that increases fluid density for better wellbore stability and sealing micro-fractures to minimize the fluid loss. Both polyanionic cellulose PAC-R and PAC-L at 1% were fluid-loss additives that stabilized the shale by maintaining it as a thin, low-permeability filter cake. Potassium chloride at 5% served to stabilize water-sensitive shales by forming stronger bonds in place of the weaker bonds of the clay structure, thus reducing water absorption and potential swelling. SiO_2 nanoparticles and MWCNT (0.05%-0.25% concentration) filled pores improve rheology and thermal stability by improving fluid viscosity with a shale swell prevention characteristic. Protective film formation through ionic liquid [OMIM]+[Cl]-(0.03%-0.11%) in shale surface leads to a significant reduction of water intrusion, thereby increasing the lubricity and provides high temperature stability. Formaldehyde is added at a concentration of 0.1% to maintain the fluid stability and prevent the growth of microbes, preventing bacterial byproducts that might degrade the fluid. Such an additive mix maintains all properties of drilling fluids to promote shale stability, cuttings transport, and thermal stability for drilling operations.

This combination of components creates the robust, high-performance, water-based drilling fluid optimized in challenging shale formations. For every component, there is also a vital role in building fluid stability, rheology, and shale inhibition plus environmental and operational concerns.

2.5. Preparation of water-based drilling fluid

Sample 1: Base fluid (WBM)

Water, XC Polymer, $CaCO_3$, PAC-R, PAC-L, PGS, KCl and Formaldehyde are used to prepare the Base fluid Sample 1 with the concentrations mentioned in Table 1.

2.6. Preparation of nano water-based drilling fluid

Table 2. Composition of Samples with Base Fluid (WBM) and Nanoparticles (SiO_2, MWCNT)

Sample 2	Base fluid + SiO_2 (0.05%)
Sample 3	Base fluid + SiO_2 (0.15%)
Sample 4	Base fluid + SiO_2 (0.25%)
Sample 5	Base fluid + MWCNT (0.05%)
Sample 6	Base fluid + MWCNT (0.15%)
Sample 7	Base fluid + MWCNT (0.25%)

Table 2 systematically lists the composition breakdown of each sample for analysis in experiments. The base fluid, WBM is progressively modified with varied concentrations of Silicon Dioxide nanoparticles and Multi-Walled Carbon Nanotubes. SiO_2 and MWCNT are used as nanoparticle additives with three levels of concentration at 0.05%, 0.15%, and 0.25% in order to analyze the effect of each one on the fluid's stability, rheology, and filtration control. Additionally, the ionic fluid is mixed with a set of samples having increasing concentrations of 0.03%, 0.05%, 0.07%, 0.09%, and 0.11% along with SiO_2 or MWCNT to study the synergy in improving shale inhibition and fluid performance. The Table 3 below presents the various formulations for the different samples. For all of them, there is a water-based base fluid (WBM) along with 0.25% concentration of either SiO_2 or MWCNT nanoparticles, with varying concentrations of an ionic fluid of between 0.03% and 0.11%. The formulation is undertaken to identify the influences which may be brought on due to changes in the nature of the nanoparticle along with the concentration of the ionic fluid concerning rheology of drilling fluids.

Table 3. Composition of Samples with Base Fluid (WBM), Nanoparticles and Ionic Liquid (SiO_2, MWCNT, and Ionic Fluid)

Sample 8	Base fluid + SiO_2 (0.25%) + Ionic fluid (0.03%)
Sample 9	Base fluid + MWCNT (0.25%) + Ionic fluid (0.03%)
Sample 10	Base fluid + SiO_2 (0.25%) + Ionic fluid (0.05%)
Sample 11	Base fluid + MWCNT (0.25%) + Ionic fluid (0.05%)
Sample 12	Base fluid + SiO_2 (0.25%) + Ionic fluid (0.07%)
Sample 13	Base fluid + MWCNT (0.25%) + Ionic fluid (0.07%)
Sample 14	Base fluid + SiO_2 (0.25%) + Ionic fluid (0.09%)
Sample 15	Base fluid + MWCNT (0.25%) + Ionic fluid (0.09%)

Sample 16	Base fluid + SiO_2 (0.25%) + Ionic fluid (0.11%)
Sample 17	Base fluid + MWCNT (0.25%) + Ionic fluid (0.11%)

2.7. Experimental Setup and Testing Procedures

Laboratory tests were performed for evaluating the performance of the nanoparticle-ionic liquid drilling fluids. Rheological testing using a viscometer on samples at simulated downhole conditions to determine the viscosity and the yield stress in high-pressure and high-temperature conditions. Grace M3600 Viscometer was utilized to measure plastic viscosity and yield point of mud samples, following standard API protocols (API RP 13B-1, 2023). The filtration tests for fluid loss were also made with a measurement of volume of filtrate for specific pressure and time. Dead Weight API Filter Press by Fann, Texas, USA was used to measure filtrate loss. To determine filtrate loss, a pressure of 100 psi, was applied for a total of 30 minutes at room temperature, to the mud samples contained in a cylindrical cup.

Based on the Bingham Plastic Model, equations (1) and (2) was used to determine the plastic viscosity (PV), and yield point (YP) (Growcock & Harvey, 2004):

$$PV = \theta_{600} - \theta_{300} \quad (1)$$

$$YP = \theta_{300} - PV \quad (2)$$

Where θ is the viscometer dial reading at N RPM (°); PV is plastic viscosity (cp); YP is yield point (lbs/100ft2); θ_{600} is dial reading at 600 RPM; and θ_{300} is dial reading at 300 RPM.

3. Results and discussion

3.1. XRD and SEM Analysis

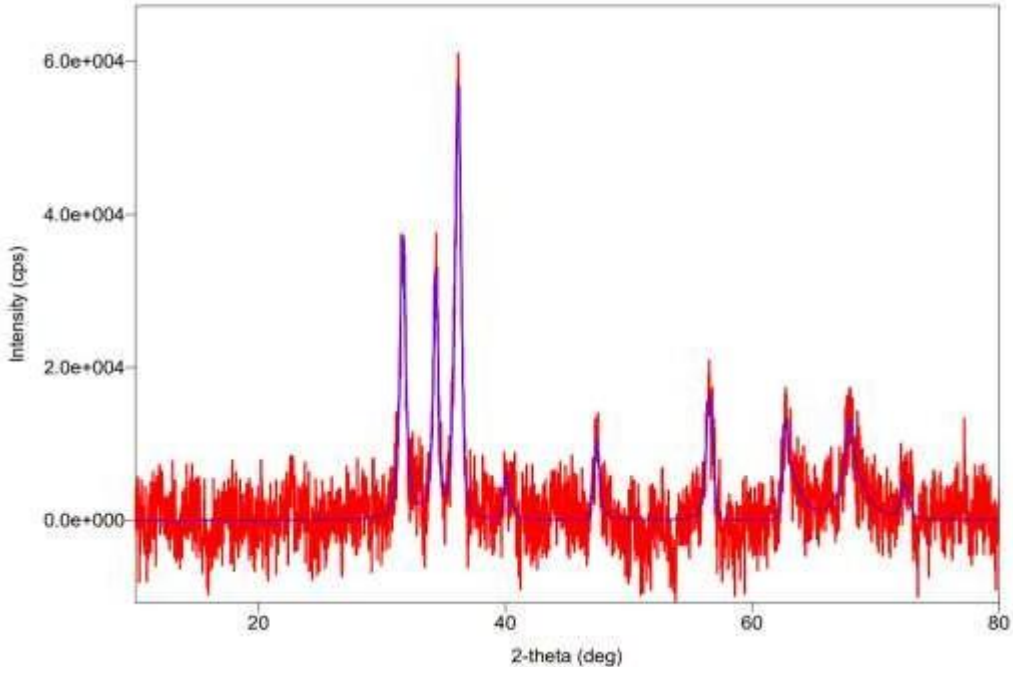

Figure 2: XRD pattern of SiO_2 Nanoparticles

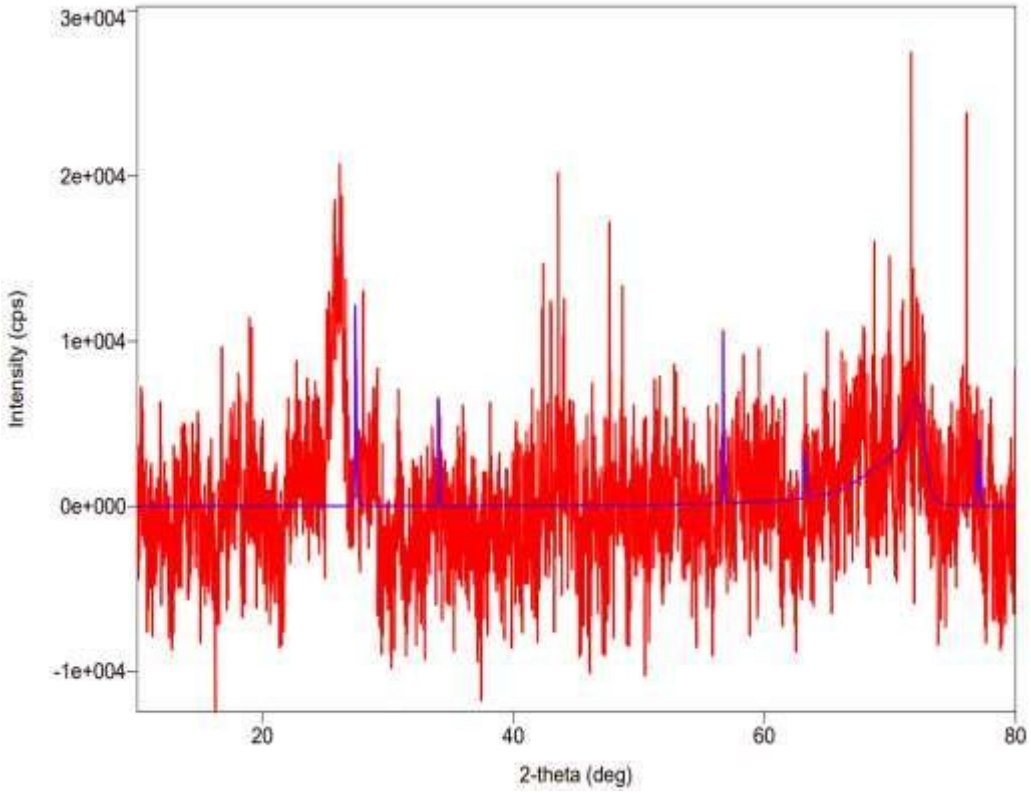

Figure 3: XRD pattern of MWCNT

Figure 2 shows the XRD pattern of SiO_2 nanoparticles, with peaks located at 31.68°, 34.29°, 36.149°, 40.04°, 47.39°, 56.466°, 62.64°, 67.88°, 72.18°. Figure 3 shows the XRD pattern of MWCNT, with peaks located at 27.403°, 34.03°, 56.697°, 63.21°, 72.1°, 76.98°.

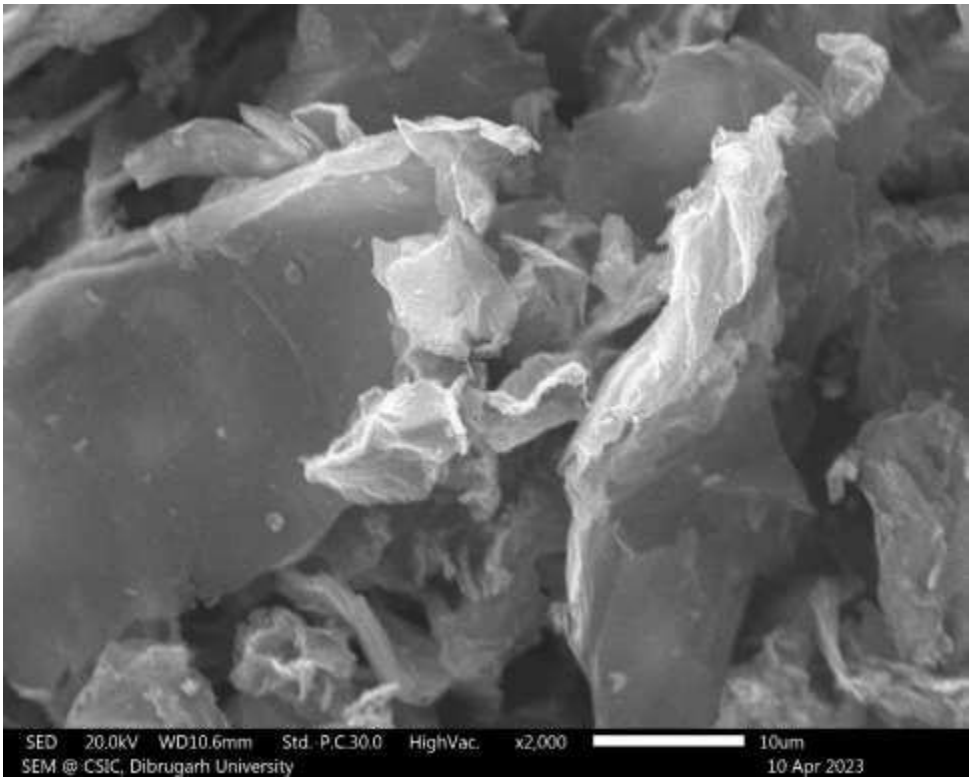

Figure 4: SEM pictures of SiO_2 nanoparticles

Figure 4 shows the SEM images of SiO_2 nanoparticles. From the images it can be seen that most of the particles are in the range of 100nm. They are mostly spherical with some amount of rough edges.

3.2. Mud Density, Filtration Loss and Mud Cake Thickness

Table 4: Density data from Mud Balance

Samples	PPG	Gm/CC	Lb/feet^3	Lb/inch^2/1000 ft
Sample 1	9.2	1.10	69.00	475.000
Sample 2	9.0	1.08	67.32	467.550
Sample 3	8.9	1.07	66.58	462.355
Sample 4	8.8	1.05	66.00	460.000
Sample 5	9.2	1.10	69.00	475.000

Sample 6	9.2	1.10	69.00	475.000
Sample 7	9.1	1.09	68.07	472.745

Table 4 shows various mud samples density obtained on a mud balance; its values are reported as: PPG, grams/cubic centimeter-Gm/CC, pound per cubic foot-Lb/fees^3 and Lb/inch^2/1,000ft. Sample 1, at a density of 9.2 PPG, or 1.10 Gm/CC, is 69 Lb/feet^3 and 475 Lb/inch^2/1,000 ft, which can be said to be rather high, thus helping keep the stability of the wellbore. Samples 2, 3, and 4 are slightly lesser in their densities, the lowest value being that of Sample 4 at 8.8 PPG, or 1.05 Gm/CC, and this may show a lighter mud formulation best suited to minimize formation damage in particular drilling conditions. Samples 5 and 6 have the same density as Sample 1, meaning either the samples are the same or at least their composition was aimed at the same level. Sample 7 was at 9.1 PPG (1.09 Gm/CC) less than Sample 1, but still of enough weight to keep the well-drilled straight. The above variations allow further comparison in the mud weight and how formulation variations impact not only formation pressure balance but ensure adequate cuttings transports.

Table 5: Dead Weight Filter Press data

Samples	Filtration loss (mL)	Mud cake thickness (mm)
Sample 1	12.2	2
Sample 2	11.8	2.1
Sample 3	10.0	2.1
Sample 4	9.6	2.4
Sample 5	12.2	2.1
Sample 6	10.8	2.1
Sample 7	10.2	2.2

Table 5 shows the results of dead weight filter press test: filtration loss in mL and mud cake thickness in mm for different fluid samples. The filtration loss that is the volume of fluid being filtered out through the mud, and the mud cake thickness which measures the thickness of the residual layer left on the filter are also the critical parameters in performance evaluation of drilling fluids. Sample 1, which has a filtration loss of 12.2 mL and a mud cake thickness of 2 mm, presents the highest fluid loss among other samples. Sample 2 has a slightly decreased filtration loss but at 11.8 mL and a marginally thicker mud cake at 2.1 mm. Samples with smaller filtration losses, like Sample 4 (9.6 mL) and Sample 7 (10.2 mL), have slightly thicker mud cakes, with Sample 4 having the thickest cake at 2.4 mm. This pattern might be a trade-off between filtration loss and thickness of the mud cake: small filtration losses are related to larger mud cakes, likely due to the more solid filter cake that decreases fluid loss. These results indicate that Samples 3, 4, 6, and 7, which have undergone lower filtration losses ranging from 9.6 to 10.8 mL and had moderate mud cake thicknesses, may offer better filtration control along with cake stability, advantages for wellbore stability in drilling applications.

3.3. Plastic viscosity, Yield point and Gel strength

Table 6: Plastic Viscosity and Yield Point

Samples	Plastic Viscosity (Centipoise)	Yield Point (lbs/100ft^2)
Sample 1	42.3	132.8
Sample 2	50.4	134.0
Sample 3	58.8	134.2
Sample 4	63.4	134.8
Sample 5	45.6	132.6
Sample 6	48.3	133.1
Sample 7	52.9	133.8

Table 6 Summary of plastic viscosity and yield point for seven samples measured in centipoise (cP) and lbs/100ft^2 respectively. Plastic viscosity (PV) is the resistance of a fluid to flow under applied stress. It is sensitive to solid content and particle interactions in the fluid. YP shows the fluid's ability to establish and sustain particle suspension in the fluid. Thus, it shows its ability for cuttings lifting during drilling operations. Out of the samples taken for consideration in the study, Sample 4 shows the highest PV, that is, 63.4 cP. In this case, high PV will take place inside the fluid due to greater resistance to flow, and such high viscosity fluids are considered very useful for cleaning purposes while drilling. Sample 3 takes the second position where the PV was calculated as 58.8 cP. Samples 1 and 5 have reasonably lower plastic viscosities at 42.3 cP and 45.6 cP, which could be easier to pump but might have a lower carrying capacity. The yield point for each sample is the same, and all samples show similar values scattered slightly between 133-135 lbs/100ft^2, which shows that all samples have consistent high suspensibility. The yield points are similar; although the plastic viscosities are different, both fluids have about the same suspension ability. This test fluid having higher values of plastic viscosity as well as yield point could be optimal for application involving good resistance to flow coupled with stability in suspending particle.

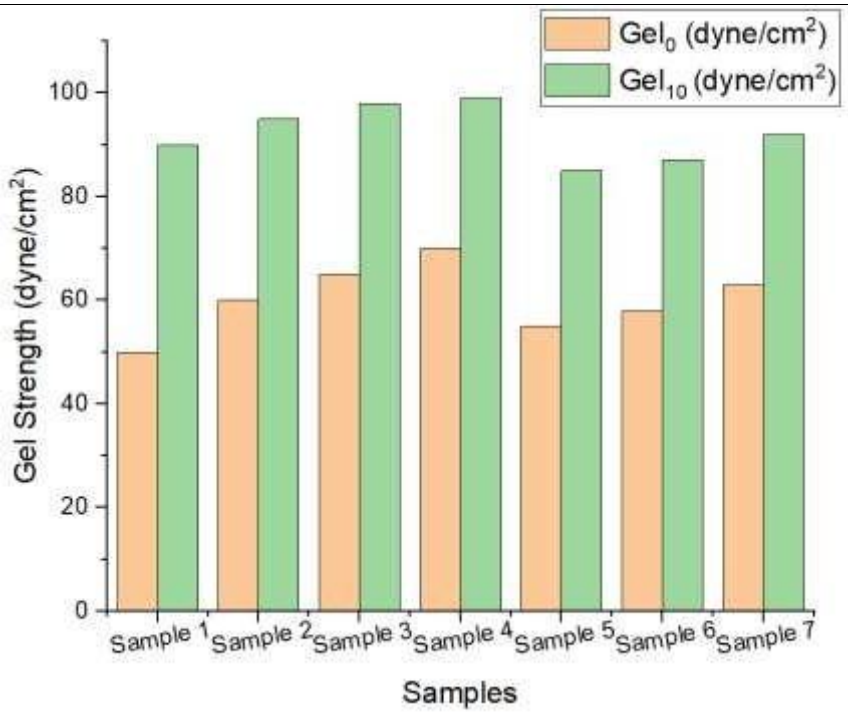

Figure 5: Gel Strength observations

Figure 5 shows the Gel strengths for seven samples; initial gel strength and gel strength after ten minutes in dyne/cm². Gel strength is defined as the ability of the drilling fluid to suspend cuttings and weighting materials when the fluid is not flowing. For effective cuttings suspension during circulation pauses, higher values are generally desirable. Sample 4 shows the highest gel strength with an initial Gel_0 of 70 dyne/cm² while Gel_{10} is at 99 dyne/cm², which means the ability to suspend suspended particles is strong for a long period. Sample 3 stands second with an initial Gel_0 of 65 dyne/cm² while Gel_{10} is 98 dyne/cm². On the other hand, Sample 1 had the lowest gel strengths: Gel_0 was 50 dyne/cm² and Gel_{10} was 90 dyne/cm². These indicated that it was relatively weaker compared to the other samples. For all samples, the values of Gel_{10} are higher than Gel_0, meaning that the structure of the gel builds strength with time when the fluid is resting and this is good for preventing settling of cuttings during interruptions in drilling. Generally, the results show that samples 3 and 4, which have the highest gel strength, are more likely to be suitable for applications that require stronger particle suspension. Sample 1 may be appropriate for conditions with minimum suspension requirements.

3.4. Characterization of 1-methyl-3-octylimidazolium chloride [OMIM]+[Cl]- (Ionic fluid)

3.4.1. Hydrogen 1 Nuclear Magnetic Resonance (NMR) Spectroscopy

This analytical technique is used to determine the structure of organic compounds by analyzing the hydrogen atoms, or protons, in a molecule. In ^{1}H NMR, a sample is placed in a very strong

magnetic field, such that the nuclear spins of the protons align either with or against the magnetic field. When radiofrequency radiation is applied, some protons flip their nuclear spins and absorb energy during this flip. This means that the resulting signal can be considered a spectrum that has peaks at different chemical shifts corresponding to a different environment of protons in a molecule. Position at which each peak occurred gives information about the nature of the hydrogen environment while its intensity, or integration, gives the number of protons in that environment. Splitting patterns, otherwise known as spin-spin coupling, give information on the number of other protons located nearby, giving information on the connectivity and the structure of the molecule.

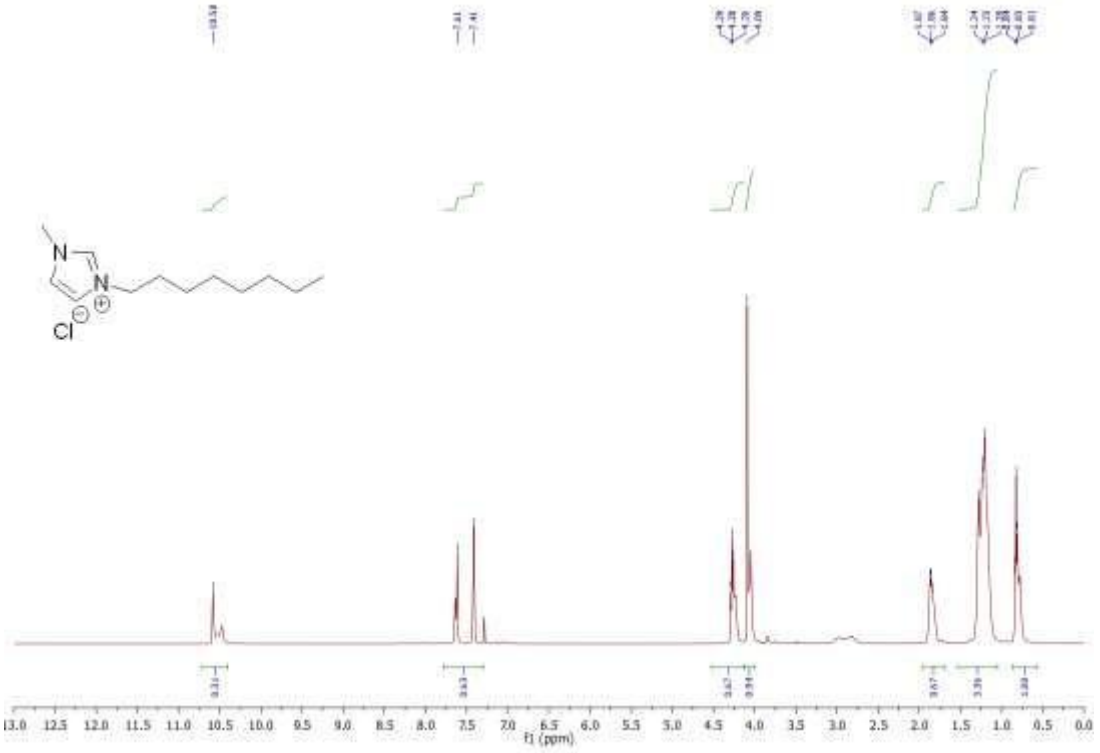

Figure 6: 1H spectra of [OMIM]+[Cl]-

^{1}H NMR (500 MHz, CDCl3) δ 10.58 (s, 1H), 7.61-7.41 (d, J = 99.3 Hz, 2H), 4.29 (t, J = 7.4 Hz, 2H), 4.09 (s, 3H), 1.87 – 1.84 (m, 2H), 1.24 – 1.20 (m, 10H), 0.84 (t, J = 6.9 Hz, 3H).

3.4.2. Carbon 13 Nuclear Magnetic Resonance (NMR) Spectroscopy

Carbon-13 Nuclear Magnetic Resonance Spectroscopy is an analytical method for determining the structure of organic compounds by focusing attention on the carbon atoms of a molecule. It does not involve the use of hydrogen, unlike ^{1}H NMR spectroscopy, but rather carbon-13, the stable yet less abundant isotope of carbon (about 1% of natural carbon).

In ^{13}C NMR, the sample is placed in a magnetic field and radiofrequency radiation is applied to make the carbon-13 nuclei absorb energy and resonate. The spectrum that results will give peaks for each and every distinct carbon environment present in the molecule. Position of each peak, that is, chemical shift informs about the electronic environment present around each carbon atom to identify functional groups and structural features. Because carbon-13 atoms are less sensitive than hydrogen atoms, signals tend to be weaker and therefore require more scans to provide a clear spectrum. But ^{13}C NMR is very useful in structural analysis because it reveals much more detail about the carbon backbone of organic molecules.

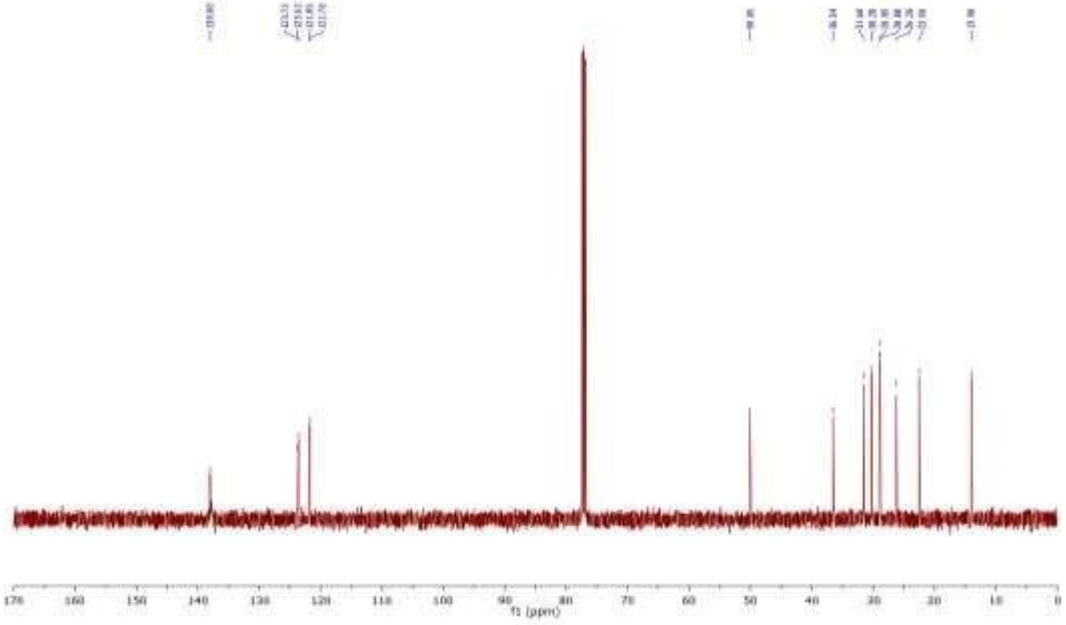

Figure 7: 13C spectra of [OMIM]+[Cl]-

^{13}C NMR (125 MHz, CDCl3) δ 138.00, 123.67, 121.82, 50.05, 36.54, 31.60, 30.28, 28.92, 26.20, 22.50, 13.98.

3.5 Rheological Properties

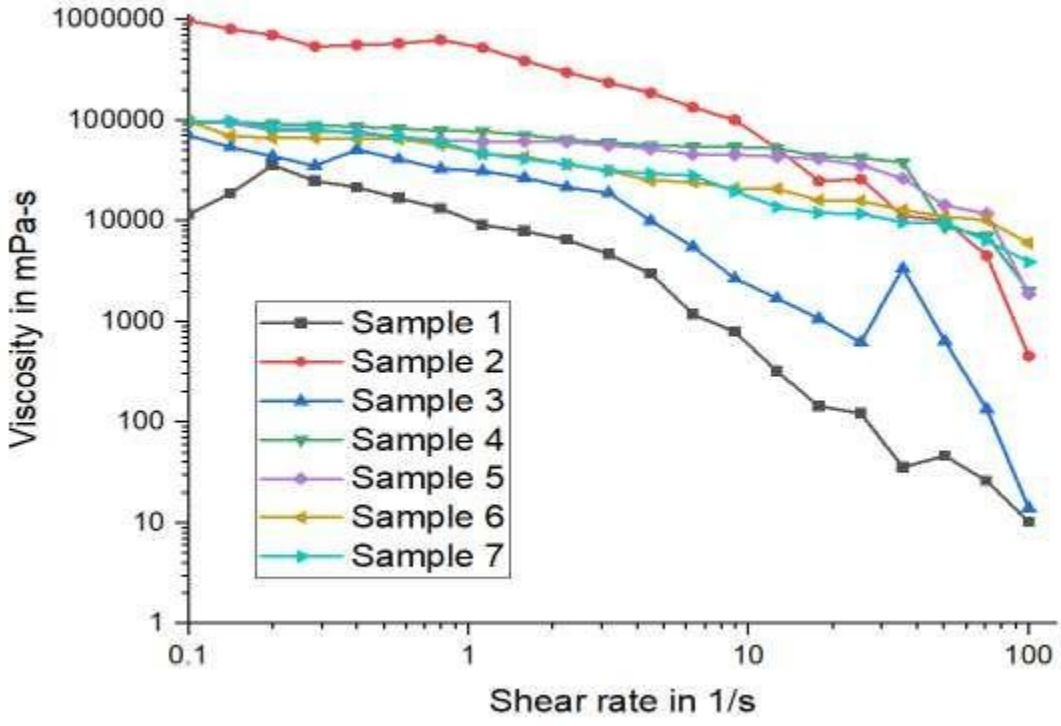

Figure 8: Viscosity Vs Shear Rate for Base fluid and Base fluid with Nanoparticles

Figure 8 shows the viscosity of base fluid and mixtures with nanoparticles versus shear rate. Shear rate is shown on the x-axis in 1/s and the y-axis is viscosity in mPa·s on logarithmic scale. There are seven samples in total that present rheological behavior. Sample 1, which is the base fluid, shows a sharp fall in viscosity with shear rate and exhibits shear-thinning behavior. Samples with the nanoparticles (Samples 2–7) show increased viscosities throughout the range of shear rates investigated and tend to have less of a drop in the viscosity profile as the shear rate increases. This implies that nanoparticles improve viscosity and diminish shear-thinning, which might be through the effect of stabilizing the nanoparticles on fluid structures under shear conditions. Stronger viscosity in samples treated with nanoparticles would be highly useful in applications where one requires fluids that do not significantly degrade properties at relatively high shearing rates.

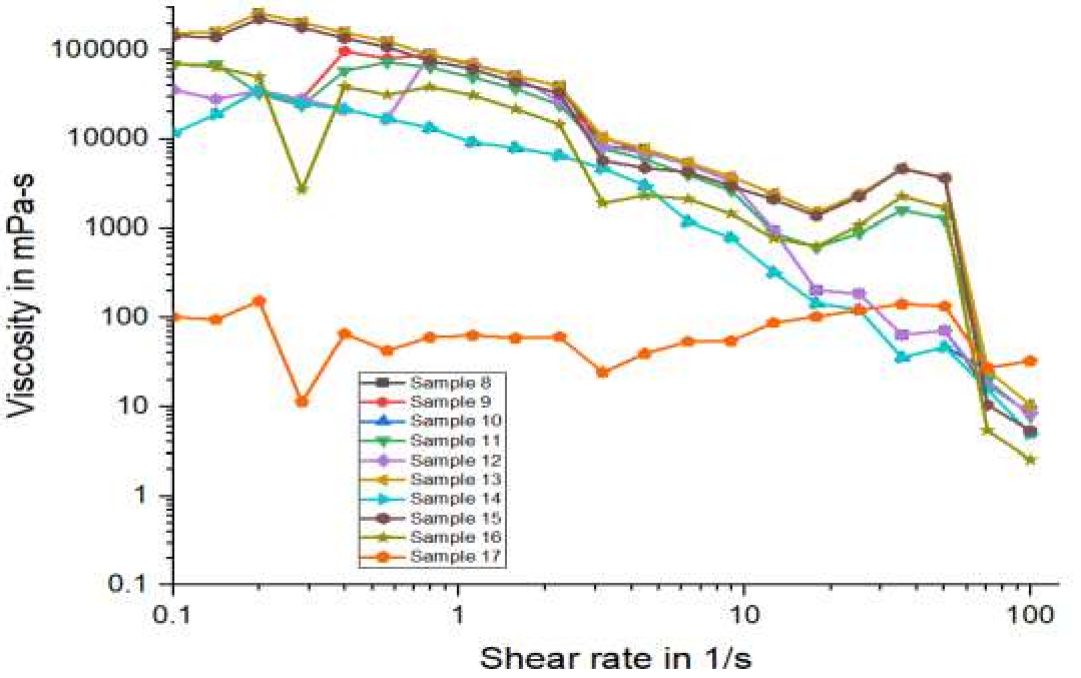

Figure 9: Viscosity Vs Shear rate for Base fluid mixed with Nanoparticles and Ionic fluid

Figure 9 shows the viscosity vs. shear rate curve of the base fluid, nanoparticles and ionic fluid mixture. A plot of different samples, 8–17, at various shear rates is provided. Samples with the nanoparticles and ionic liquids show different viscosity profiles against the shear rate range of most samples, which will decrease viscosity with an increasing shear rate. Such behavior is beneficial when the attenuation of viscosity at higher rates of shear is desired for providing a better flow when higher viscosities need to be maintained at a lower shear rate to stabilize particle suspension and hole cleaning in drilling applications. Significantly lower viscosity in Sample 16 indicates that the other samples have a different rheological property characteristic, possibly due to either different concentration or type of ionic fluid or nanoparticle. Different types of viscosity profiles among samples may be suggestive of tuning capabilities in the composition of nano-particles and ionic fluid to match specific operational needs.

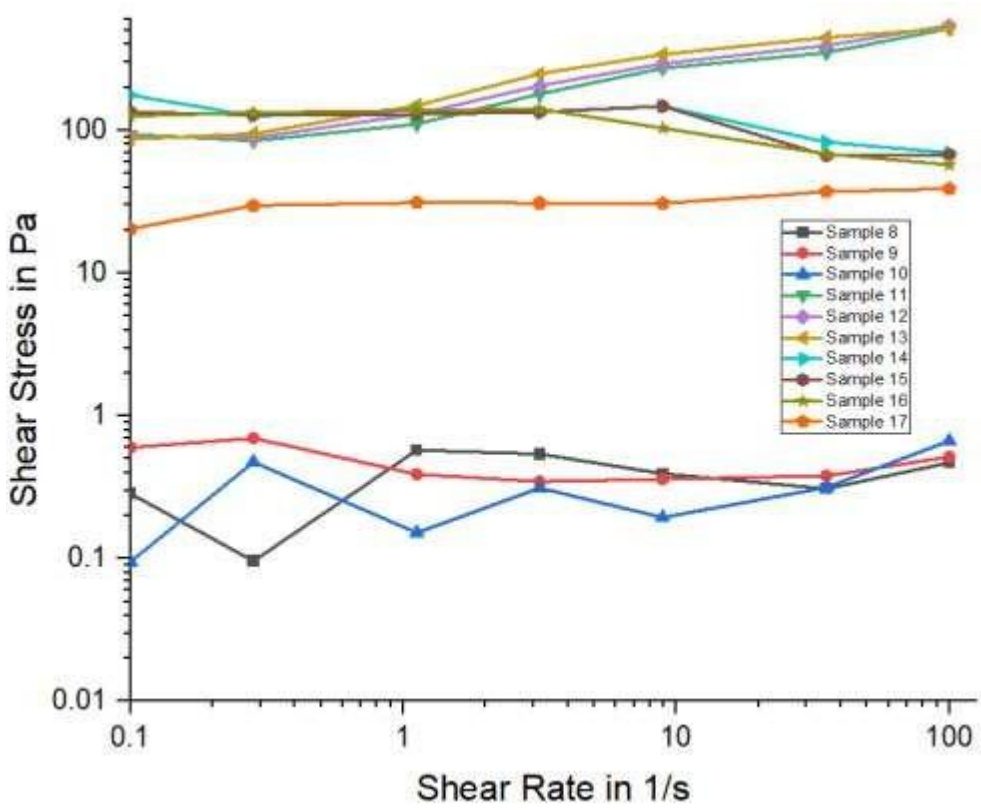

Figure 10: Shear Stress Vs Shear rate for Base fluid mixed with Nanoparticles and Ionic fluid

Figure 10 demonstrates shear stress and shear rate graph for the base fluid mixed with nanoparticles and ionic fluid. Most samples have shear stresses of relatively constant values which respond only weakly to increases in shear rate, approximating Newtonian fluid behaviour. Other samples show greater values as Sample 16, representing greater values that indicate more resistance in flowing, a feature probably linked with their higher concentration or type of nanoparticles or ionic fluid added that also adds strength in the structures. This uniform shear stress at various shear rates in some samples indicates that these formulations may be capable of stable performance under various shear conditions, and hence have the potential applicability to the drilling environment where the fluid should have stable and predictable behavior with varying flow rates. Variability of samples points toward the versatility of adjusting shear stress properties of the fluid through the variation of composition and concentration of nanoparticles and ionic fluids. The lowest shear rate in 0.1 1/s was at: Sample 8, with shear stress at 0.286 Pa; Sample 9, with 0.60189 Pa; and Sample 10 with 0.09531 Pa. Samples 11 through 16, on the other hand, show the highest shear stresses with approximately 87.13 Pa for Sample 13 down to 177.06 Pa for Sample 14, thus showing more resistance to deformation. Sample 17, however, displays an intermediate shear stress value of 20.462 Pa at this low shear rate. With increasing shear rate, the shear stress is expected to

increase with more marked increases at higher initial values, for example, Sample 11 to Sample 13 reached above 500 Pa at 100 1/s. For instance, from an initial value of about 87.131 Pa in Sample 13, it increased up to nearly 518.44 Pa at the maximum shear rate. Interestingly, some samples show more stable or slightly decreasing trends at higher shear rates; Sample 16, for example, starts at 126.43 Pa at 0.1 1/s and slightly drops to 57.527 Pa at 100 1/s, showing a drop in shear stress with an increase in shear rate. Sample 14 shows some interesting trends: it has a maximum at lower shear rates of 134.74 Pa at 0.1 1/s and goes down to 69.878 Pa at 100 1/s, suggesting the possibility of shear thinning.

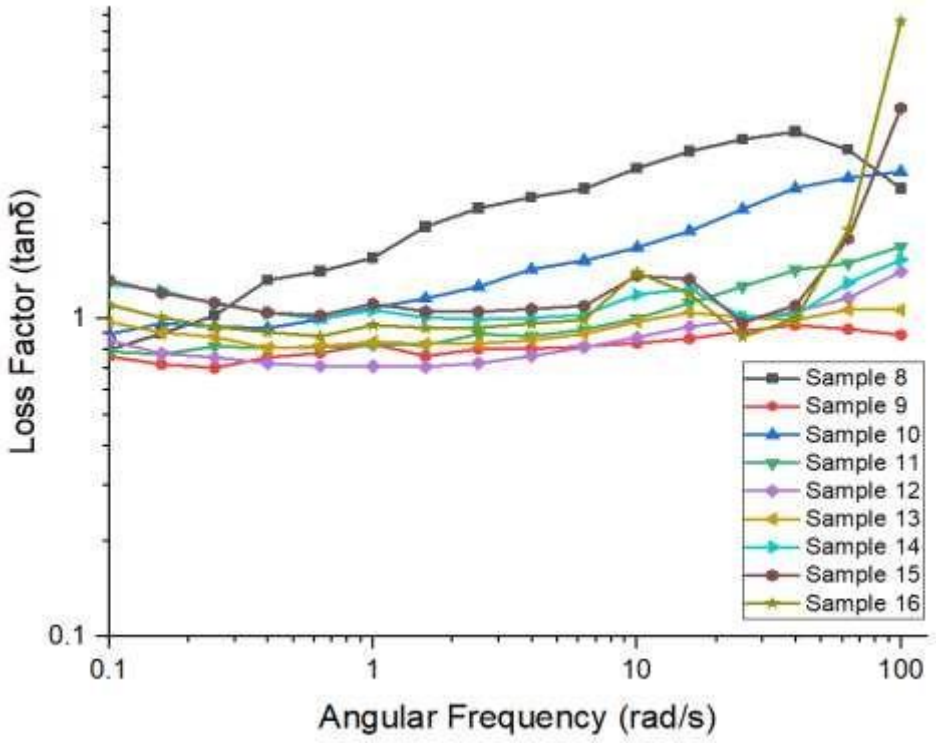

Figure 11: Loss Factor Vs Angular frequency for Base fluid mixed with Nanoparticles and Ionic fluid

Figure 11 represents the variation of loss factor, tan δ with respect to angular frequency for samples prepared by blending base fluid with nanoparticles and with ionic fluids. The loss factor is the ratio of viscous to elastic components. Hence, for values greater than 1, the material is more viscous, and vice versa for values less than 1. Most samples show stable tan δ values lying between or above 1 in the frequency range. Samples 8 and 10 exhibit an increase in tan δ with frequency, meaning the fluid exhibits higher viscous behavior at higher frequencies, and Sample 13 displays a peak at high frequencies that indicate a viscosity shift to elevated shear rates. These results indicate that nanoparticle and ionic fluid concentrations can significantly alter the rheological properties of the base fluid in the presence of specific drilling conditions.

4 Conclusion

This paper investigated the nanoparticle and ionic liquid-enhanced base fluids for the drilling of shale formations, focusing on their rheology. The nanoparticles in the base fluid would also maintain viscosity at low shear rates but lower it at high shear rates, leading to some preferred shear-thinning behavior. This behavior makes it possible for effective cuttings suspension at low flow rates while cutting down the pumping energy requirements at the higher shear rates. The addition of nanoparticles to ionic liquids provides a means for fine-tuning the viscosity and stability of these fluids over a wide range of shear rates, allowing for fine-tuning over a wide range of drilling specificities. The fluids thus obtained can be stabilized under a range of downhole pressures and temperatures to achieve optimal flow through fragile shale formations. Shear stress-shear rate analysis showed that some samples exhibited near-Newtonian behaviour, while others built up resistance to stress, and therefore tailored fluid composition for known downhole stresses. Such synergy of nanoparticles and ionic liquids can therefore enhance shale drilling efficiency, minimize the loss by the damage of formation, and minimize fluid loss risks.

Disclosure statement

The authors report there are no competing interests to declare.

Funding

No funding was received.

Acknowledgment

Sincere thanks are extended by the authors to Dibrugarh University's Department of Chemistry, Department of Petroleum Technology, and Department of Petroleum Engineering for providing the access of institutional facilities and resources needed to complete the work, without which it would not have been feasible.

References

1. Aftab, A., Ismail, A. R., & Ibupoto, Z. H. (2017). Enhancing the rheological properties and shale inhibition behavior of water-based mud using nanosilica, multi-walled carbon nanotube, and graphene nanoplatelet. Egyptian Journal of Petroleum, 26(2), 291–299. https://doi.org/10.1016/j.ejpe.2016.05.004
2. API RP 13B-1. (2023). Field Testing Water-based Drilling Fluids. May 2019.
3. Bayat, A. E., & Shams, R. (2019). Appraising the impacts of SiO2, ZnO and TiO2 nanoparticles on rheological properties and shale inhibition of water-based drilling muds. Colloids and Surfaces A: Physicochemical and Engineering Aspects, 581, 123792. https://doi.org/10.1016/j.colsurfa.2019.123792
4. Blkoor, S. O., & Ka, F. (2013). The Influence of XC-Polymer on Drilling Fluid Filter Cake Properties and Formation Damage. 4(5). https://doi.org/10.4172/2157-7463.1000157
5. Gao, C. H. (2024). Drilling fluids for shale fields : Case studies and lessons learnt. Unconventional Resources, 4(November 2023), 100070. https://doi.org/10.1016/j.uncres.2023.100070
6. Growcock, F., & Harvey, T. (2004). Drilling Fluids. In Drilling Fluids Processing Handbook (pp. 15–68). Elsevier. https://doi.org/10.1016/B978-075067775-2/50003-2

7. Ismail, A. R., Aftab, A., Ibupoto, Z. H., & Zolkifile, N. (2016). The novel approach for the enhancement of rheological properties of water-based drilling fluids by using multi-walled carbon nanotube, nanosilica and glass beads. Journal of Petroleum Science and Engineering, 139, 264–275. https://doi.org/10.1016/j.petrol.2016.01.036
8. Kamali, F., Saboori, R., & Sabbaghi, S. (2021). Fe3O4-CMC nanocomposite performance evaluation as rheology modifier and fluid loss control characteristic additives in water-based drilling fluid. Journal of Petroleum Science and Engineering, 205(December 2020), 108912. https://doi.org/10.1016/j.petrol.2021.108912
9. Lundegard, P. D., & Samuels, N. D. (1980). Field classification of fine-grained sedimentary rocks. Journal of Sedimentary Petrology, 50(3), 781–786. https://doi.org/10.1306/212F7E14-2B24-11D7-8648000102C1865D
10. Luo, Z., Pei, J., Wang, L., Yu, P., & Chen, Z. (2017). Influence of an ionic liquid on rheological and filtration properties of water-based drilling fluids at high temperatures. Applied Clay Science, 136, 96–102. https://doi.org/10.1016/j.clay.2016.11.015
11. Muhammed, N. S., Olayiwola, T., Elkatatny, S., Haq, B., & Patil, S. (2021). Insights into the application of surfactants and nanomaterials as shale inhibitors for water-based drilling fluid: A review. Journal of Natural Gas Science and Engineering, 92(May), 103987. https://doi.org/10.1016/j.jngse.2021.103987
12. Ofei, T. N., Bavoh, C. B., & Rashidi, A. B. (2017). Insight into ionic liquid as potential drilling mud additive for high temperature wells. Journal of Molecular Liquids, 242, 931–939. https://doi.org/10.1016/j.molliq.2017.07.113
13. Rahman, M. T., Negash, B. M., Moniruzzaman, M., Quainoo, A. K., Bavoh, C. B., & Padmanabhan, E. (2020). An Overview on the potential application of ionic liquids in shale stabilization processes. Journal of Natural Gas Science and Engineering, 81(July), 103480. https://doi.org/10.1016/j.jngse.2020.103480
14. Talukdar, P. (2017). Use of Reservoir and Environment Friendly Bio-Polymers in the Reservoir Drilling Fluid of Upper Assam Basin. 10(7), 169–180.
15. Talukdar, P., & Gogoi, S. B. (2015). A Study on the Role of Pre-Gelatinized Starch (PGS) in the Non Damaging Drilling Fluid (NDDF) for the Tipam Sand of Geleki Oilfield of Upper Assam Basin. International Journal of Applied Sciences and Biotechnology, 3(2), 291–300. https://doi.org/10.3126/ijasbt.v3i2.12552
16. Talukdar, P., Kalita, S., Pandey, A., Dutta, U., & Singh, R. (2018). Effectiveness of different Starches as Drilling Fluid Additives in Non Damaging Drilling Fluid. International Journal of Applied Engineering Research, 13(16), 12469–12474. http://www.ripublication.com
17. Xia, P., & Pan, Y. (2023). Effects of nanosilica on the properties of brine-base drilling fluid. Scientific Reports, 13(1), 1–13. https://doi.org/10.1038/s41598-023-47932-w
18. Zou, C., Zhu, R., Chen, Z. Q., Ogg, J. G., Wu, S., Dong, D., Qiu, Z., Wang, Y., Wang, L., Lin, S., Cui, J., Su, L., & Yang, Z. (2019). Organic-matter-rich shales of China. Earth-Science Reviews, 189, 51–78. https://doi.org/10.1016/j.earscirev.2018.12.002